

# Dynamic observation of the behavior of 3 keV $D_2^+$ irradiated into $Li_2O$ using IR absorption spectroscopy

Takuji Oda <sup>a,\*</sup>, Yasuhisa Oya <sup>b</sup>, Satoru Tanaka <sup>a</sup>

<sup>a</sup> Department of Quantum Engineering and Systems Science, The University of Tokyo, 7-3-1 Hongo, Bunkyo-ku, Tokyo 113-8565, Japan

<sup>b</sup> Radioisotope Center, The University of Tokyo, 2-11-16 Yayoi, Bunkyo-ku, Tokyo 113-0032, Japan

Received 12 October 2004; accepted 12 July 2005

## Abstract

In order to understand the influence of radiation defects on hydrogen isotope behavior in  $Li_2O$ , an in situ IR absorption analysis was carried out during 3 keV  $D_2^+$  irradiation. Three IR absorption peaks were obtained from the stretching vibrations of O–Ds in different existence states: an O–D existing as a LiOD phase at  $2710\text{ cm}^{-1}$ , a surface O–D with several adjacent O–Ds at  $2660\text{ cm}^{-1}$ , and an O–D affected by a defect in the bulk at  $2605\text{ cm}^{-1}$ . At the outset of the irradiation, only the surface O–D appeared. As the ion fluence increased, the O–D affected by a defect started to form in the bulk, and the LiOD phase followed it. The defect related with the O–D at  $2605\text{ cm}^{-1}$  was regarded as a Li vacancy. It was indicated that the hydrogen isotopes were stabilized in  $Li_2O$  through an interaction with the Li vacancy ( $LiO^-D^+$ :  $2605\text{ cm}^{-1}$ ) or mutual aggregation (LiOD phase:  $2710\text{ cm}^{-1}$ ).

© 2005 Elsevier B.V. All rights reserved.

PACS: 61.80.Jh; 78.30.–j

## 1. Introduction

The interaction of hydrogen isotopes with radiation defects is one of the most influential factors determining the tritium inventory in a fusion blanket. This influence is enhanced during the operation of a fusion reactor, due to the increase in defect concentration. Therefore, an understanding of this influence is important for establishing a secure and efficient fuel cycle.

Lithium oxide ( $Li_2O$ ) is a candidate material for a solid breeder, and many experimental studies have focused on the influence of radiation defects on hydro-

gen isotope behavior in  $Li_2O$  [1]. Among various radiation defects, Li vacancies and F centers have attracted considerable attention, because the former are extensively generated via the tritium breeding reaction and the latter are recognized to strongly affect the stability [2,3] and the charge state [4–6] of tritium. The generation and annihilation behaviors of these defects were investigated under/after neutron/ion irradiation in various conditions [7–12], and the influences on tritium diffusivity were deduced based on the connection with the results of previous tritium release experiments [13–17]. However, the reliability of these approaches is insufficient owing to the difficulty in controlling all parameters determining the tritium release rate. Indeed, the tritium diffusion coefficients acquired in these tritium release experiments were widely scattered across a few orders of magnitude [4,13–17].

\* Corresponding author. Tel.: +81 3 5841 6970; fax: +81 3 3818 3455.

E-mail address: [oda@flanker.q.t.u-tokyo.ac.jp](mailto:oda@flanker.q.t.u-tokyo.ac.jp) (T. Oda).

In the last 10 years, quantum chemical calculations have been employed in order to appraise the specific influences of each defect. The stability of the hydrogen isotopes interacting with Li vacancies [18] or F centers [19,20] has been evaluated. The calculated influence of the F centers was in good agreement with the experimental results, while the calculated influence of the Li vacancies differed from the experimental results; tritium migration was depressed by the Li vacancies according to the calculation [18], whereas it seemed to be suppressed in the experiment [21]. This discrepancy may have derived from the low reliability of the deduction based on the tritium release experiments. Hence, the present study aims to directly observe the interaction of hydrogen isotopes with radiation defects, without relying on the tritium release experiments.

For this purpose, IR absorption spectroscopy was employed. This technique can identify the existence states of hydrogen isotopes in metal oxides [22], because O–H, which is a major chemical form of hydrogen isotopes, exhibits multiple IR absorption peaks reflecting the surrounding conditions, such as the proximate existence of a defect. In the case of  $\text{Li}_2\text{O}$ , several O–D peaks have been reported both on the surface [23,24] and in the bulk [25–28], and some of them have been assigned to O–Ds interacting with point defects [24,26]. In the present study, the IR absorption analysis was combined with the ion implantation technique, and an in situ measurement was performed during 3 keV  $\text{D}_2^+$  irradiation. The deuterium ion irradiation introduces not only deuterium, but also radiation defects into the same region simultaneously. Hence, frequent interaction of the hydrogen isotopes with the radiation defects is induced, and clear observation of the interaction is expected.

## 2. Experimental

A  $\text{Li}_2\text{O}$  single crystal grown by the floating zone method [29] was cut into a disk with a diameter of 10 mm and a thickness of 1 mm, for use as the sample. Fig. 1 depicts a schematic drawing of the experimental system for the in situ IR absorption analysis during 3 keV  $\text{D}_2^+$  irradiation. This system consists of an FT-IR (Mattson, Infinity Gold), an ion gun, a sample heating and cooling unit, and a vacuum chamber. Prior to a series of experiments, the sample was annealed in a heating furnace under  $1 \times 10^{-4}$  Pa at 1173 K for 6 h in order to decompose impurities such as LiOH and  $\text{Li}_2\text{CO}_3$ . Subsequently, the sample was transferred to the vacuum chamber with a sample holder made of molybdenum, and the vacuum chamber was evacuated to  $1 \times 10^{-6}$  Pa. For the elimination of the impurities formed near the surface region during the sample transfer, the sample was re-annealed at 923 K until the IR absorption peaks related with LiOH and  $\text{Li}_2\text{CO}_3$  disappeared. The

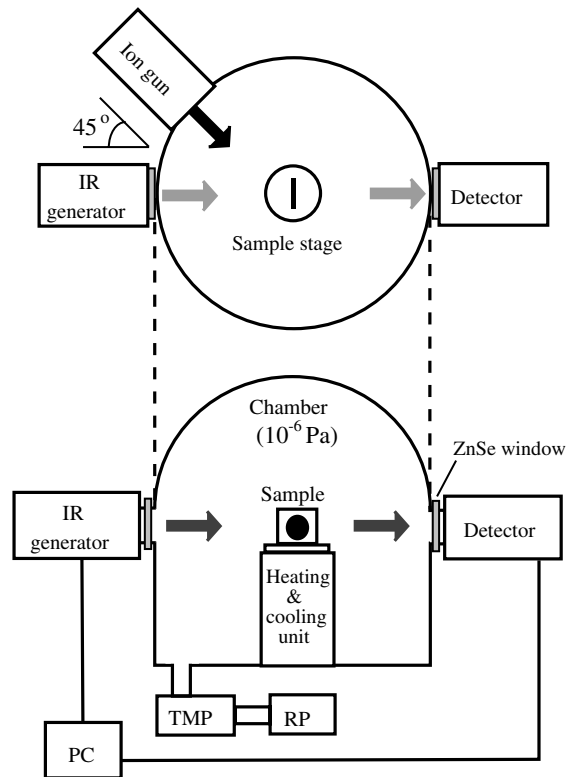


Fig. 1. Schematic drawing of the IR absorption analysis system combined with an ion gun.

residual amount of H in  $\text{Li}_2\text{O}$  was considered to be less than  $10^{-9}$  H/ $\text{Li}_2\text{O}$ , based on the solubility of H [30], on the assumption that all of the residual gas at  $1 \times 10^{-6}$  Pa is  $\text{H}_2$ .

After this pretreatment,  $\text{D}_2$  gas was introduced into the chamber at  $3 \times 10^{-3}$  Pa for the  $\text{D}_2^+$  irradiation. The surface normal of the sample was irradiated with 3 keV  $\text{D}_2^+$  at an angle of  $45^\circ$ , and an in situ IR absorption analysis was performed. The incident angle of the IR light was  $0^\circ$ . According to the TRIM calculation, 1.5 keV  $\text{D}_2^+$  corresponding to 3 keV  $\text{D}_2^+$  induces 10 vacancies/ion, and the average doped depth is 32 nm. The ion flux was adjusted to  $0.6 \times 10^{17}$   $\text{D}_2^+$   $\text{m}^{-2}$   $\text{s}^{-1}$  using a Faraday cup. The sample temperature was measured by a K-type thermocouple attached on the sample surface. During the ion irradiation, the sample temperature increased to around 313 K. The parameters of the IR absorption analysis were set to a resolution of  $2 \text{ cm}^{-1}$ , a measurement range of  $4000\text{--}1000 \text{ cm}^{-1}$ , and an integral number of scans of 2000, in order to ensure a sufficient S/N ratio. The measurement of one spectrum took 13 min. The recorded spectra were converted to the absorbance format, using the spectrum before the irradiation as the reference. It is known that an area of a peak in the absorbance format is proportional to the concentration of the

chemical species absorbing the IR light. Consequently, we were able to explore the variations in the concentration of O–Ds in various existence states as a function of the ion fluence.

### 3. Results and discussion

Regarding the chemical form of the hydrogen isotopes in  $\text{Li}_2\text{O}$ , five types are conceivable:  $-\text{OH}^-$ ,  $\text{H}^0$  and  $\text{H}^-$  captured by the F centers, LiH, and hydrogen bubbles. As reported in Refs. [4,5], the main chemical state of the hydrogen isotopes introduced by thermal absorption or neutron irradiation is  $\text{T}^+$  forming  $-\text{OT}^-$ . A few tens % of  $\text{T}^-$  was observed only in the case of neutron irradiation, and it was attributed to  $\text{T}^-$  captured by the F centers [5].  $\text{T}^0$  was negligible in the both reported cases [5]. As for the Li colloids, which seem to generate LiH, the formation was not induced by the ion irradiation, but by high-fluence electron irradiation ( $10^{23}$ – $10^{24}$   $\text{cm}^{-2}$ ) [31,32]. Hydrogen bubbles were not observed after the neutron irradiation, whereas helium bubbles were detected [33]. Based on these facts, we considered that the main existence state of the implanted deuterium was  $\text{D}^+$  existing as  $-\text{OD}^-$ , and the discussion was focused only on  $-\text{OD}^-$ . However, it should be noted that since some deuterium could exist in the other chemical forms and they cannot be detected by IR absorption spectroscopy, behavior of these deuterium is one of the uncertainties in the present study.

A typical IR absorption spectrum is shown in Fig. 2, recorded during the 3 keV  $\text{D}_2^+$  irradiation at an ion flu-

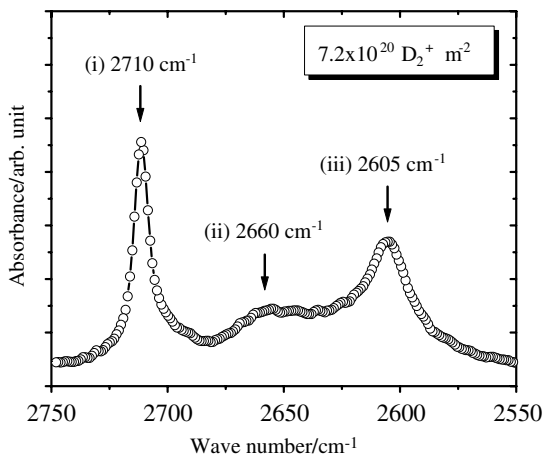


Fig. 2. The typical IR absorption spectrum of  $\text{Li}_2\text{O}$  during 3 keV  $\text{D}_2^+$  irradiation, with a flux of  $0.6 \times 10^{17}$   $\text{D}_2^+$   $\text{m}^{-2}$   $\text{s}^{-1}$  up to a fluence of  $7.2 \times 10^{20}$   $\text{D}_2^+$   $\text{m}^{-2}$  at 313 K (i) 2710  $\text{cm}^{-1}$ , an O–D existing as a LiOD phase; (ii) 2660  $\text{cm}^{-1}$ , a surface O–D with several adjacent O–Ds; and (iii) 2605  $\text{cm}^{-1}$ , an O–D affected by a defect in the bulk.

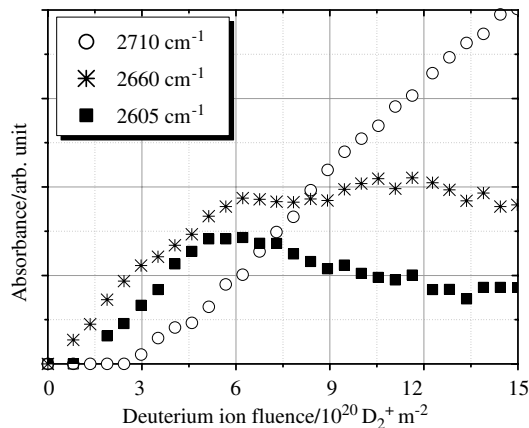


Fig. 3. Variations of the peak area of the each O–D as a function of ion fluence during 3 keV  $\text{D}_2^+$  irradiation with a flux of  $0.6 \times 10^{17}$   $\text{D}_2^+$   $\text{m}^{-2}$   $\text{s}^{-1}$  at 313 K.

ence of  $7.2 \times 10^{20}$   $\text{D}_2^+$   $\text{m}^{-2}$ . Three IR absorption peaks originating from the O–D stretching vibrations were observed at the wave numbers 2710  $\text{cm}^{-1}$ , 2660  $\text{cm}^{-1}$  and 2605  $\text{cm}^{-1}$ . By comparison with the literature, these peaks were attributed to the following O–Ds: an O–D existing as the LiOD phase at 2710  $\text{cm}^{-1}$  [17], a surface O–D with several adjacent O–Ds at 2660  $\text{cm}^{-1}$  [14], and an O–D affected by a defect in the bulk at 2605  $\text{cm}^{-1}$  [15]. The broadness of the 2660  $\text{cm}^{-1}$  peak was caused by the variety in the existence states of surface O–Ds and the effect of the hydrogen bonds among them. It should be noted that no clear peak was found at the O–H region, although small or broad peaks were difficult to detect with the present experimental setup due to the influence of the O–H in the air on the IR path.

The area variations of each peak are given in Fig. 3 as a function of the ion fluence up to  $1.5 \times 10^{21}$   $\text{D}_2^+$   $\text{m}^{-2}$ . The area of the peak at 2710  $\text{cm}^{-1}$  and 2605  $\text{cm}^{-1}$  was individually evaluated by fitting with a Lorentz-type function, after the subtraction of the proper background. In the case of the peak at 2605  $\text{cm}^{-1}$ , since its shape was too broad to estimate the area directly by the same fitting procedure, the area was figured out by subtraction of the summed area of the peaks at 2710  $\text{cm}^{-1}$  and 2605  $\text{cm}^{-1}$  from the area at 2750–2550  $\text{cm}^{-1}$  including all three peaks. Hereafter, we discussed the behavior of the implanted deuterium ions by dividing the ion fluence range into low (below  $1 \times 10^{20}$   $\text{D}_2^+$   $\text{m}^{-2}$ ), middle (from  $1 \times 10^{20}$  to  $3 \times 10^{20}$   $\text{D}_2^+$   $\text{m}^{-2}$ ), and high (above  $3 \times 10^{20}$   $\text{D}_2^+$   $\text{m}^{-2}$ ).

#### 3.1. Low fluence range ( $< 1 \times 10^{20}$ $\text{D}_2^+$ $\text{m}^{-2}$ )

In this fluence range, only the surface O–D at 2660  $\text{cm}^{-1}$  was clearly observed, whereas the O–Ds in the bulk at 2710  $\text{cm}^{-1}$  and 2605  $\text{cm}^{-1}$  were largely undetected.

Even in a high vacuum, such as that of the present experiment,  $\text{Li}_2\text{O}$  reacts with residual water, and the surface is rapidly covered with O–Hs [34]. Hence, the formation of the surface O–D by the  $\text{D}_2^+$  irradiation was considered to be due to three processes mainly: the sputtering of the surface O–Hs, the movement of the implanted deuterium from the bulk to the surface, and the trapping of the deuterium by activated sites on the surface. Additionally, the isotope exchange reaction between the surface O–Hs and the atmospheric  $\text{D}_2/\text{D}_2\text{O}$  or  $\text{D}^+$  diffused from the bulk, and the adsorption of atmospheric  $\text{D}_2\text{O}$  during the  $\text{D}_2^+$  irradiation might have contributed. However, the contribution of the isotopic exchange with the atmospheric  $\text{D}_2/\text{D}_2\text{O}$  seemed to be small, because surface O–D peaks did not appear before the irradiation, even though the sample was placed in  $3 \times 10^{-3}$  Pa of  $\text{D}_2$ . An interesting point is the scant appearance of bulk O–Ds at the outset of the irradiation, which indicates that the implanted deuterium that exists as  $\text{D}^+$  is not effectively kept in the bulk when the defect concentration is low. Based on the rapid formation of the surface O–D as shown in Fig. 3, it is reasonable to assume that some implanted deuterium moved to the surface quickly, which resulted in the formation of surface O–Ds.

### 3.2. Middle fluence range ( $1 \times 10^{20}$ – $3 \times 10^{20}$ $\text{D}_2^+ \text{m}^{-2}$ )

When the fluence reached  $1 \times 10^{20}$   $\text{D}_2^+ \text{m}^{-2}$ , the O–Ds affected by defects ( $2605 \text{ cm}^{-1}$ ) started to increase non-linearly with increasing ion fluence, prior to the appearance of the LiOD phase ( $2710 \text{ cm}^{-1}$ ), as shown in Fig. 4.

The formation of the O–D affected by a defect requires not only deuterium but also defects in the bulk. Therefore, the non-linear increase of the O–D at  $2605 \text{ cm}^{-1}$  was attributed to a double role of the deute-

rium ion irradiation, i.e., the introduction of the deuterium and the generation of the defect. The broadness of the peak was considered to result from the crystalline distortion induced by the irradiation. The defect related to this O–D at  $2605 \text{ cm}^{-1}$  could be assigned to the Li vacancy, because (i) the number of Li vacancies formed by the ion irradiation could be higher than that of O vacancies [35], and (ii) the predominant formation of the LiOD phase ( $2710 \text{ cm}^{-1}$ ) by  $\text{D}_2$  thermal absorption and the generation of the peak at  $2605 \text{ cm}^{-1}$  by the quenching technique have been reported [26]; this is similar to the case of  $\text{MgO}:\text{Mg}(\text{OH})_2$  precipitates were minimized and  $\text{V}_{\text{OH}}^-$  ( $\text{H}^+$  substitutional for  $\text{Mg}^{2+}$ ) was maximized by the quenching technique [36].

The absence of an O–D in the bulk in the low fluence range and the appearance of the  $2605 \text{ cm}^{-1}$  peak in the middle fluence range were observed. These results imply that the deuterium that exists as  $\text{D}^+$  cannot stay in the bulk under conditions of low defect concentration. In other words, interstitial  $\text{D}^+$  ( $\text{Li}_2\text{O}-\text{D}^+$ ) is thermally unstable enough to migrate at room temperature, and it can be stabilized by the interaction with a Li vacancy, namely through the formation of  $\text{LiO}^--\text{D}^+$  at  $2605 \text{ cm}^{-1}$ . This hypothesis is consistent with the reported results of quantum chemical calculations, in which the diffusion barrier of  $\text{H}^+$  in the  $\text{Li}_2\text{O}-\text{H}^+$  was estimated to be 0.45 eV, and that in the  $\text{LiO}^--\text{H}^+$  0.98 eV [18,37].

### 3.3. High fluence range ( $> 3 \times 10^{20}$ $\text{D}_2^+ \text{m}^{-2}$ )

The LiOD phase emerged last among the three peaks at  $3 \times 10^{20}$   $\text{D}_2^+ \text{m}^{-2}$ . The surface O–D and the O–D affected by defects stopped increasing at  $6 \times 10^{20}$   $\text{m}^{-2}$ . Above this fluence, the O–D affected by defects decreased and only the LiOD phase increased continuously.

As the surface area of the sample is limited, it is reasonable to assume that the surface O–D becomes saturated. The relationship between the saturation fluence of  $6 \times 10^{20}$   $\text{D}_2^+ \text{m}^{-2}$  and the conceivable surface O–D concentration of about  $1 \times 10^{19}$  O–D  $\text{m}^{-2}$ , estimated based on the surface structure, can be accounted for, if the surface sputtering yield of 5% for H in LiOH under 1.5 keV  $\text{D}^+$  is considered, based on the TRIM calculation. This fact would constitute evidence that the formation of surface O–D is initiated by the surface sputtering.

The formation of the LiOD phase is induced by the aggregation of O–Ds. Hence, a high concentration of O–Ds is necessary for the formation of this phase. In the present experiment, the appearance of the peak at  $2710 \text{ cm}^{-1}$  followed the formation of  $\text{LiO}^--\text{D}^+$ , as shown in Fig. 3, because stable O–Ds in  $\text{Li}_2\text{O}$  were mainly  $\text{LiO}^--\text{D}^+$  when they were not aggregated. The formation of the LiOD phase could therefore be described as follows:

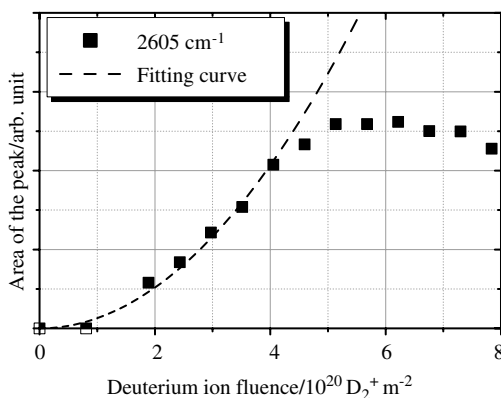


Fig. 4. Detailed behavior of the O–D affected by a defect ( $2605 \text{ cm}^{-1}$ ) at the beginning of the irradiation.

$(\text{LiO}^- - \text{D}^+)_n \rightarrow \text{LiOD phase}$ .

The number of  $\text{LiO}^- - \text{D}^+$  enough to form the LiOD phase is not clear at this point. According to this reaction equation, the formation of the LiOD phase occurs with the coincidental decrease of  $\text{LiO}^- - \text{D}^+$  when the concentration of  $\text{LiO}^- - \text{D}^+$  reaches a level high enough to enable its aggregation. After the formation of a certain amount of the LiOD phase, direct absorption of the implanted deuterium by the LiOD phase is likely to additionally contribute to the formation of the LiOD phase, which would then accelerate. These phenomena were observed above  $6 \times 10^{20} \text{ D}_2^+ \text{ m}^{-2}$  in the form of a saturation and decrease of  $\text{LiO}^- - \text{D}^+$  and a steep increase in the LiOD phase. These results indicate that hydrogen isotopes are stabilized in the bulk not only through the interaction with the Li vacancies ( $\text{LiO}^- - \text{D}^+$ ), but also through mutual aggregation (LiOD phase). This aggregation behavior has also been observed in our previous work [27], where the peak at  $2605 \text{ cm}^{-1}$  faded away at 363 K, with a contrary increase of the peak at  $2710 \text{ cm}^{-1}$ .

Finally, we want to mention some uncertain points in the present study for future studies. One uncertainty is behavior of the Li and the O that were knocked out from their ideal, although many Li vacancies seemed to be formed. The formation of large number of Li vacancies could be ascribed to the selective sputtering, and to the preferential replacement of Li by the irradiation, as compared with the O defect. Indeed, a large difference exists in the defect formation energies of Frenkel pair between Li (2.5 eV) and O (9 eV), according to the potential models reported in Ref. [38]. Another uncertainty is the charge state of the irradiated region. In the present experimental conditions, deuterium was mainly implanted as  $\text{D}_2^+$ . Hence, the irradiated region could be charged positively. The charge state is also varied by the formations of F centers, Li colloids, hydrogen and oxygen bubbles, and the recoils/releases of Li, O, D,  $\text{D}_2$  and  $\text{D}_2\text{O}$ , etc. In order to deepen the discussion by settling those uncertainties in future studies, an atomic-scale understanding of the irradiation behavior of  $\text{Li}_2\text{O}$  itself is important.

#### 4. Conclusions

In order to understand the influence of radiation defects on hydrogen isotope behavior in  $\text{Li}_2\text{O}$ , in situ IR absorption analyses were conducted during 3 keV  $\text{D}_2^+$  irradiation. Three IR peaks of the O–D stretching vibration were observed: a LiOD phase at  $2710 \text{ cm}^{-1}$ , surface O–Ds at  $2660 \text{ cm}^{-1}$ , and an O–D interacting with a Li vacancy, namely  $\text{LiO}^- - \text{D}^+$  at  $2605 \text{ cm}^{-1}$ . The area variations of each peak as a function of ion fluence indicated that the hydrogen isotopes were stabilized in the bulk

through the interaction with the Li vacancies ( $\text{LiO}^- - \text{D}^+$ :  $2605 \text{ cm}^{-1}$ ) or through mutual aggregation (LiOD phase:  $2710 \text{ cm}^{-1}$ ). It was confirmed that the Li vacancies delayed the migration of the hydrogen isotopes. For the precise prediction of tritium behavior, it is important to include the influence of the Li vacancies, because many Li vacancies are generated via the nuclear reaction under real reactor conditions.

#### References

- [1] A. Donato, *Fus. Eng. Des.* 38 (1998) 369.
- [2] Y. Asaoka, H. Moriyama, Y. Ito, *Fus. Technol.* 21 (1992) 1944.
- [3] V. Grishmanov, S. Tanaka, J. Tiliks, G. Kizane, A. Supe, T. Yoneoka, *Fus. Eng. Des.* 39&40 (1998) 685.
- [4] H. Kudo, K. Okuno, *J. Nucl. Mater.* 133&134 (1985) 192.
- [5] K. Okuno, H. Kudo, *J. Nucl. Mater.* 138 (1986) 31.
- [6] H. Moriyama, A. Okada, Y. Asaoka, Y. Ito, *J. Nucl. Mater.* 179–181 (1991) 839.
- [7] K. Noda, K. Uchida, T. Tanifuji, S. Nasu, *Phys. Rev. B* 24 (1981) 3736.
- [8] K. Noda, Y. Ishii, H. Matsui, H. Watanabe, *J. Nucl. Mater.* 133–134 (1985) 205.
- [9] Y. Asaoka, H. Moriyama, K. Iwasaki, K. Moritani, Y. Ito, *J. Nucl. Mater.* 183 (1991) 174.
- [10] S. Tanaka, D. Yamaki, M. Yamawaki, T. Miyamura, R. Kiyose, *Fus. Eng. Des.* 28 (1995) 292.
- [11] V. Grishmanov, S. Tanaka, T. Terai, *J. Nucl. Mater.* 246 (1997) 126.
- [12] V. Grishmanov, S. Tanaka, T. Yoneoka, *J. Nucl. Mater.* 248 (1997) 128.
- [13] K. Okuno, H. Kudo, *J. Nucl. Mater.* 116 (1983) 82.
- [14] D. Guggi, H.R. Ihle, D. Bruning, U. Kurz, S. Nasu, K. Noda, T. Tanifuji, *J. Nucl. Mater.* 118 (1983) 100.
- [15] T. Tanifuji, K. Noda, T. Takahashi, H. Watanabe, *J. Nucl. Mater.* 149 (1987) 227.
- [16] T. Terai, Y. Takahashi, S. Tanaka, *Fus. Eng. Des.* 7 (1989) 345.
- [17] T. Kurasawa, H. Watanabe, *J. Nucl. Mater.* 179–181 (1991) 851.
- [18] R. Shsh, A.D. Vita, V. Heine, M.C. Payne, *Phys. Rev. B* 53 (1996) 8257.
- [19] H. Tanigawa, S. Tanaka, *J. Nucl. Mater.* 307–311 (2002) 1446.
- [20] H. Tanigawa, S. Tanaka, *Fus. Eng. Des.* 61&62 (2002) 789.
- [21] H. Kudo, *Radiochim. Acta* 50 (1990) 71.
- [22] W. Wohlecke, L. Kovacs, *Crit. Rev. Solid State Mater. Sci.* 25 (2001) 1.
- [23] S. Tanaka, M. Taniguchi, M. Nakatani, D. Yamaki, M. Yamawaki, *J. Nucl. Mater.* 218 (1995) 335.
- [24] S. Tanaka, M. Taniguchi, *J. Nucl. Mater.* 248 (1997) 101.
- [25] T. Kurasawa, V.A. Maroni, *J. Nucl. Mater.* 119 (1983) 95.
- [26] H. Tanigawa, S. Tanaka, *Fus. Eng. Des.* 51&52 (2000) 193.
- [27] T. Oda, Y. Oya, S. Tanaka, *J. Nucl. Mater.* 329–333 (2004) 1256.
- [28] S. Tanaka, T. Oda, Y. Oya, *J. Nucl. Mater.* 329–333 (2004) 1270.

- [29] I. Shindo, S. Kumura, K. Noda, T. Kurasawa, S. Nasu, J. Nucl. Mater. 79 (1979) 418.
- [30] H. Katsuta, S. Konishi, H. Yoshida, J. Nucl. Mater. 116 (1983) 244.
- [31] P. Vajda, F. Beuneu, G. Krexner, M. Prem, O. Blaschko, C. Majer, Nucl. Instrum. and Meth. B 166&167 (2000) 275.
- [32] P. Vajda, F. Beuneu, J. Nucl. Mater. 258–263 (1998) 495.
- [33] R.A. Verrall, D.H. Rose, J.M. Miller, I.J. Hastings, D.S. MacDonald, J. Nucl. Mater. 855–858 (1991) 179.
- [34] T. Oda, H. Tanigawa, S. Tanaka, Fus. Sci. Technol. 44 (2003) 485.
- [35] N. Ando, M. Akiyama, Y. Oishi, J. Nucl. Mater. 95 (1980) 259.
- [36] Y. Chen, M.M. Abraham, H.T. Tohver, Phys. Rev. Lett. 37 (1976) 1757.
- [37] R. Shah, A.D. Vita, M.C. Payne, J. Phys. Condens. Mat. 7 (1995) 6981.
- [38] J.G. Rodeja, M. Meyer, M. Hayoun, Model. Simul. Mater. Sci. Eng. 9 (2001) 81.